Catalysis Letters, Vol. 117, Nos. 3–4, September 2007 (© 2007)
DOI: 10.1007/s10562-007-9118-5

Effect of calcination behaviors on precipitated iron–manganese Fischer–Tropsch synthesis catalyst

Zhichao Tao,[a,b] Yong Yang,[a] Mingyue Ding,[a,b] Tingzhen Li,[a,b] Hongwei Xiang,[a,*] and Yongwang Li[a]

[a]*State Key Laboratory of Coal Conversion, Institute of Coal Chemistry, Chinese Academy of Sciences, Taiyuan, 030001, P.R. China*
[b]*Graduate University of Chinese Academy of Sciences, Beijing, 100039, P.R. China*

Received 3 April 2007; accepted 3 April 2007

Calcination behaviors play an important role in Fischer–Tropsch (FT) performance over a slurry iron–manganese catalyst. The present study was undertaken to investigate the effects of calcination behaviors (calcination temperature, heating rate and calcination atmosphere) on the textural properties, reduction/carburization behavior, bulk phase structure and FT synthesis performances over precipitated Fe–Mn catalysts. N_2 physisorption, X-ray photoelectron spectroscopy (XPS), H_2 thermal gravimetric analysis (TGA) and Mössbauer effect spectroscopy (MES) were used to characterize the catalyst. It is found that increasing calcination temperature and heating rate lead to low surface area and high enrichment of Mn on the catalyst surface. High calcination temperature also increased the crystallite size of α-Fe_2O_3 and suppressed the reduction/carburization of the catalysts in H_2 and syngas. Low calcination temperature and low heating rate promoted the further carburization of the catalyst and increased the activity during FT process. High calcination temperature and low heating rate restrained the formation of CH_4, increases C_5^+ selectivity and improved the selectivity to light olefins. In addition, calcination in argon could improve the carburization and increase FT activity of the catalyst. The present iron–manganese catalyst with lower calcination temperature, lower heating rate and calcined in argon is optimized for its FT performances.

KEY WORDS: Fischer–Tropsch synthesis; iron–manganese catalyst; calcination.

1. Introduction

Fischer–Tropsch (FT) synthesis has attracted increasing industrial attention as an alternative technology to produce clean transportation fuels and chemicals from coal and natural gas [1–3]. The use of iron-based catalysts in the commercial FT process is very attractive due to their high FT activity as well as their water–gas shift (WGS) reactivity [4–6].

To elucidate factors that affect the catalytic performances (activity, selectivity and stability) of iron-based catalysts and to improve the catalysts potential capability for applications, lots of attempts have focused on the addition of promoters and the optimization of preparation conditions [7,8]. Manganese has been attracted an increasing interest as one of the promoters of iron-based catalyst due to the fact that manganese could not only act as chemical promoter to change the chemisorption of the catalyst, but also act as structural promoter to improve the dispersion of active iron and stabilize the catalyst in FT process [9–12]. It is reported that a moderate amount of manganese incorporated into iron-based catalyst could improve FT activity and selectivity to light olefins [11,13,14]. On the other hand, preparation conditions, such as calcination behaviors, also play dominant role in the structure and FT performances of the catalysts [15,16]. Rankin and Bartholomew [15,16] have investigated the effects of calcination temperature on the adsorption, chemical/physical properties and FT activity/selectivity properties of K-promoted Fe/SiO_2 catalyst. They found that the increase of calcination temperature of $Fe/K/SiO_2$ catalyst lowers its adsorption capacities for H_2 and CO, decreases its reduction degree, but does not affect its CO_2 adsorption capacity, metal particle size or potassium coverage. Moreover, the increasing calcination temperature of the catalyst leads to a decrease in FT activity and shift the products to light olefins. Huang *et al.* [17] have studied the effects of preparation conditions on the textural properties of alumina support. They found that the surface area of alumina decreases with increasing calcinations temperature. Just as for these catalysts/supports, solution of the issues related to the calcination behaviors is also very essential for iron–manganese FT catalysts. However, the studies on the effect of calcination temperature on iron–manganese FT catalyst are rarely reported. Moreover, the discussions of the effect of calcination atmosphere and heating rate on the structure and FT performances of iron–manganese catalyst are seriously lacking.

The objective of the present study is to investigate the effect of calcination temperature, heating rate and calcination atmosphere on the performances of iron–manganese catalysts in order to optimize the calcination conditions. Particular attentions are paid to

*To whom correspondence should be addressed.
E-mail: hwxiang@sxicc.ac.cn

the effect of calcination behaviors on the catalyst reduction, textural properties and the bulk phase structure of the precipitated iron–manganese catalysts as-prepared, after reduction and after FT reaction. FT activity, stability and the hydrocarbon selectivity are systematically investigated in slurry reactor and well correlated with the characterization results.

2. Experimental

2.1. Catalyst preparation

The catalysts used in this study were prepared by the combination of co-precipitated and spray drying method. The detailed preparation method has been described in elsewhere [18]. Briefly, a solution containing $Fe(NO_3)_3$ and $Mn(NO_3)_2$ with the desired ratio (the weight compositions of the two catalysts are 100Fe/12Mn and 100Fe/50Mn, respectively) was coprecipitated with NH_4OH solution as precipitator at pH = 9.0 ± 0.1 and T = 80 ± 1 °C. The precipitate was completely washed, filtered, and then spray-dried. The spray-dried powder was dried at 120 °C for 5 h, then heated to required temperature at a desired heating rate in air or argon, and finally calcined for 5 h in a muffle furnace. The obtained catalyst samples with spherical particle size of 10–20 μm were used for the application of FT reaction in slurry phase reactor. Detailed composition, calcination conditions and label of the catalysts used in this study are presented in table 1.

2.2. Catalyst characterizations

The elemental contents in the catalysts were determined by inductively coupled plasma emission spectroscopy (ICPES) using an Atomscan 16 spectrometer (TJA, USA). The surface compositions of the fresh catalysts were determined by X-ray photoelectron spectroscopy (XPS), using a PHI Quantera SXM spectrometer with AlKα radiation.

The BET surface area, pore volume and average pore size of fresh catalysts were determined via N_2 physisorption at the normal boiling point of N_2(−196 °C), using a Micromeritics ASAP 2500 instrument.

The thermogravimetric analysis (TGA) was performed using an MS OmniStar 200 instrument. Typically, 20–30 mg samples were treated in 5%H_2/Ar (on mole basis) at 100 °C for 20 min and then temperature was increased to 800 °C at a rate of 10 °C/min and held for 30 min before cooling.

Mössbauer spectroscopy was measured with a FAST Series MR-351 constant-acceleration Mössbauer spectrometer (FAST, Germany) at room temperature, using a 25 mCi ^{57}Co in Pd as γ-ray source. The spectral components were identified on the basis of their isomeric shift (IS), quadruple splitting (QS) and magnetic hyperfine field (Hhf). All isomer shift values were reported with respect to me ed with the 330 kOe field of α-Fe at room temperature.

2.3. Reactor system and operation procedure

FT performances of the catalysts were tested in a 1 dm^3 slurry phase reactor. For each test, about 20 g fresh catalyst and 320 g liquid wax were loaded in the reactor. After being reduced at 290 °C with syngas (H_2/CO = 0.67) for 24 h, the reactor system was adjusted to the required reaction conditions. The detailed description of the reactor and product analysis systems have been given elsewhere [5].

3. Results and discussions

3.1. Textural properties and reduction of the catalysts

The BET surface, pore volume, average pore size, Mn/Fe weight ratio in the bulk and the surface of the catalysts with different calcination conditions as-prepared are shown in table 1. It is apparent that increasing calcination temperature and heating rate decreases the surface area and increases the average pore size due to crystallite growth, which can be proved by Mössbauer effect spectroscopy (MES) results in the present study. At the same time, the increase of calcination temperature and

Table 1
Detailed composition, calcination conditions, label and textural properties of the catalysts as-prepared

Catalysts	C-1	C-2	C-3	C-4	C-5	C-6	C-7	C-8
Calcination temperature (°C)	300	400	500	600	500	500	500	500
Heating rate (°C/min)	2.0	2.0	2.0	2.0	0.5	2.0	5.0	2.0
Calcination atmosphere	Air	Air	Air	Air	Air	Air	Air	Ar
Mn/Fe ($\times 10^2$ weight ratio)								
Bulk	44.1	44.8	44.7	47.5	13.2	13.1	13.2	13.1
Surface	47.4	49.6	129.2	127.4	34.2	34.9	36.7	27.8
BET surface area (m^2/g)	179	163	58	15	61	48	48	50
Pore volume (cm^3/g)	0.28	0.28	0.22	0.18	0.25	0.25	0.25	0.22
Average pore size (nm)	6.27	6.78	15.27	46.31	16.21	21.26	21.06	17.19

heating rate also improves the enrichment of Mn on the catalyst surface. However, the catalyst (C-8) calcined in argon has lower enrichment degree of Mn on the catalyst surface compared with the catalyst (C-6) calcined in air.

Figure 1 displays the H_2-DTG curves of the catalysts. It is found that the peaks below 300 °C appeared in the catalysts (C-1 and C-2) with low calcination temperature disappeared with further increase of calcination temperature. They are probably due to the reduction or decomposition of residual hydroxide or nitrate which is converted to oxide with increase of calcination temperature [19]. The three negative peaks at 300–800 °C observed in DTG pattern for all catalysts represent the reduction steps of α-Fe_2O_3 to Fe_3O_4 (α-Mn_2O_3 to Mn_3O_4), Fe_3O_4 to FeO (Mn_3O_4 to MnO), and FeO to α-Fe, respectively [20,21]. All these peaks shift to higher temperature with the increase of calcination temperature. The results indicate that increasing calcination temperature suppresses the reduction of the catalysts which maybe due to the crystallite growth of α-Fe_2O_3, since the small crystallite size of α-Fe_2O_3 can be easily reduced in H_2 [16]. In addition, calcination atmosphere and heating rate have little effects on the reduction behaviors of the catalysts due to their similar crystallite size of α-Fe2O_3.

3.2. Crystallite structure of the catalysts

Bulk iron phases in catalysts as-prepared, after reduction and after reaction were detected by MES, and the results are summarized in table 2. The catalysts of C-1 and C-2 only present one doublet. According to literature [22], the doublet is typical for the superparamagnetic (spm) Fe^{3+} ions on the non-cubic sites with the crystallite diameters smaller than 13.5 nm. It is found that the crystallite size of α-Fe_2O_3 was obviously increased with increasing calcination temperature, and slightly increased with the increase of heating rate, which is well agrees with the BET and H_2-DTG results. It is also found that increasing calcination temperature and heating rate increase the hyperfine field (Hhf) value, making it come up to the α-Fe_2O_3 standard value, 515 kOe. (The Hhf value of α-Fe_2O_3 for the catalysts as-prepared C-3 to C-8 is 507, 510, 510, 512, 514 and 513 kOe, respectively.) The results indicate that increasing calcination temperature and heating rate decrease the crystal deficit of the iron oxide in the catalyst, making it come up to the α-Fe_2O_3 standard.

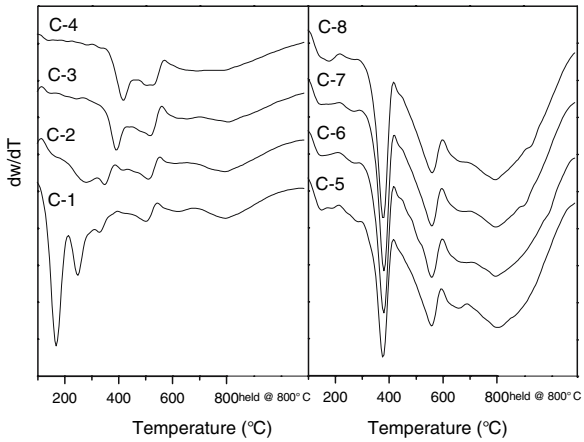

Figure 1. H_2-DTG curves of the catalysts.

Table 2 shows that it is difficult to detect the iron carbides phases from the catalysts with different calcination temperature after being reduced, which maybe due to the small crystallite size of iron carbides caused by the high interdispersion effect of manganese oxide, since the manganese content in these catalysts is very high. These catalysts are further reduced and carburized in FT process, and the content of iron carbides decreases with the increase of calcination temperature. On the other hand, appropriate increase of heating rate promotes the carburization of the catalyst after reduction, but leads to a decrease of iron carbides content in FT process, compared with the content after reduction. This can be attributed to the unstable structure of these catalysts, since partial iron carbides may be reoxidized to Fe_3O_4 by the H_2O vapor formed in the FT process [23]. In addition, the catalyst calcined in argon possesses the high carburization degree during the reduction and FT process than that calcined in air. These results can be explained by the synergetic effects of several factors. The MES and XPS results have indicated that increasing calcination temperature and heating rate increase the crystallite size of α-Fe_2O_3 and promote the enrichment of manganese on the catalyst surface, and both of them facilitate the dissociation adsorption of CO and promote the carburization of the catalysts [10,24,25]. However, the crystal deficit of α-Fe_2O_3 is decreased with the increase of calcination temperature and heating rate, which suppress the further carburization or do not stabilize the iron carbides phases of the catalysts in FT process.

3.3. Fischer–Tropsch synthesis performances

The results of the effects of calcination behaviors on catalyst activity and stability for FT reaction are shown in figure 2. It is generally accepted that the iron carbides are main active phases for the FT reaction [26,27], and the content of iron carbides determined by MES can be used to monitor the amount of FT reaction active sites to some extent. The catalyst (C-1) with low calcination temperature has lower initial activity, but the activity is increased during FT process. Increasing calcination temperature decreases FT activity, which is well agreed with the MES analysis. The catalysts (C-6 and C-8) with medium heating rate (2 °C/min) present higher initial activity, but they deactivate quickly due to the reoxidation

Table 2
Mössbauer parameters of the catalysts as-prepared, after reduction[a] and after reaction[b]

Catalysts	As-prepared		After reduction		After reaction	
	Phases	Area (%)	Phases	Area (%)	Phases	Area (%)
C-1	Fe^{3+} (spm)	100	Fe^{2+} (spm)	41.9	χ-Fe_5C_2	44.9
			Fe^{3+} (spm)	58.1	Fe_3O_4	44.2
					Fe^{3+} (spm)	10.9
C-2	Fe^{3+} (spm)	100	Fe^{2+} (spm)	42.5	χ-Fe_5C_2	16.6
			Fe^{3+} (spm)	57.5	Fe_3O_4	71.1
					Fe^{3+} (spm)	12.3
C-3	α-Fe_2O_3	79.1	Fe_3O_4	30.2	χ-Fe_5C_2	15.6
	Fe^{3+} (spm)	20.9	Fe^{2+} (spm)	48.2	Fe_3O_4	74.5
			Fe^{3+} (spm)	21.6	Fe^{2+} (spm)	9.5
					Fe^{3+} (spm)	0.4
C-4	α-Fe_2O_3	92.9	Fe_3O_4	97.8	Fe_3O_4	67.0
	Fe^{3+} (spm)	7.1	Fe^{3+} (spm)	2.2	Fe^{2+} (spm)	29.1
					Fe^{3+} (spm)	3.9
C-5	α-Fe_2O_3	88.1	χ-Fe_5 C_2	1.2	χ-Fe_5C_2	3.5
	Fe^{3+} (spm)	11.9	Fe_3O_4	90.6	Fe_3O_4	96.5
			Fe^{3+} (spm)	8.2		
C-6	α-Fe_2O_3	95.3	χ-Fe_5C_2	2.5	χ-Fe_5C_2	1.2
	Fe^{3+} (spm)	4.7	Fe_3O_4	95.6	Fe_3O_4	98.8
			Fe^{3+} (spm)	1.9		
C-7	α-Fe_2O_3	93.1	Fe_3O_4	24.4	χ-Fe_5C_2	0.7
	Fe^{3+} (spm)	6.9	Fe^{2+} (spm)	63.8	Fe_3O_4	99.3
			Fe^{3+} (spm)	11.8		
C-8	α-Fe_2O_3	97.9	χ-Fe_5 C_2	2.8	χ-Fe_5C_2	1.4
	Fe^{3+} (spm)	2.1	Fe_3O_4	96.1	Fe_3O_4	98.6
			Fe^{3+} (spm)	1.1		

[a]Reduction condition: H_2/CO = 0.67, 0.30 MPa, 290 °C and 1000 h^{-1} for 24 h.
[b]Reaction condition H_2/CO = 0.67, 1.50 MPa, 270 °C and 1000 h^{-1} for 200 h.

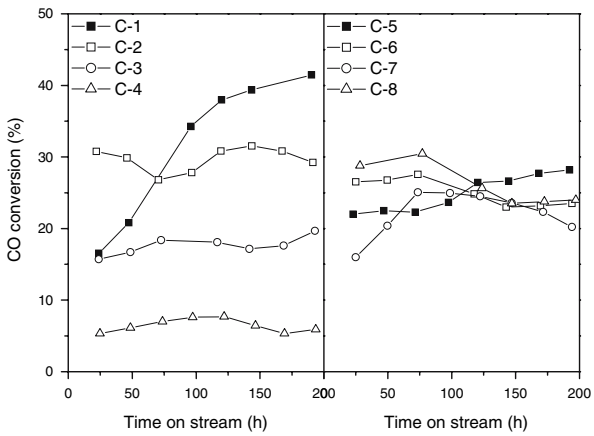

Figure 2. Carbon monoxide conversion of the catalysts. Reaction condition: H_2/CO = 0.67, 270 °C, 1.50 MPa and 1000 h^{-1} for 200 h.

of partial iron carbides to Fe_3O_4 in the process of FT process. However, the catalyst with low heating rate stabilizes the iron carbides and suppresses the reoxidation of iron carbide to Fe_3O_4, which improves further carburized of the catalysts and increases the activity during FT process. In addition, the activity of the catalyst with high heating rate firstly increases, and then decreases with time on stream, and shows lower stability.

The effects of calcination behaviors on the selectivity of hydrocarbon products and the olefin/paraffin ratio are shown in figure 3 and table 3. It is found that increasing calcination temperature suppressed the formation of CH_4 and increases the C_5^+ selectivity. The olefin/paraffin ratio in C_2–C_4 increases significantly with the increase of calcination temperature and passed through a maximum at the calcination temperature of 500 °C, and then decreases with further increase of calcination temperature. These results may be attributed to the enrichment of Mn on the catalyst surface and the increase of the crystallite size of iron phases. Barrault and Renard [10] and Jensen and Mssoth [28] had reported that manganese can promote dissociation adsorption of CO, increase the selectivity of olefin in gas phase, and shift the products to heavy hydrocarbons. Cagnoli *et al.* [25] suggested that the large iron crystal size facilitates the dissociation adsorption of CO and promotes the formation of heavy hydrocarbons. The synergetic effects of these factors result in that a high calcination temperature is favorable for the formations of heavy hydrocarbons as well as the light olefins. However, the low FT activity of the catalyst C-4 leads to the high exit H_2/CO ratio, which decreases the olefins selectivities. On the other hand, the catalyst with low heating rate has higher C_5^+ selectivity and light olefins selectivities than the catalysts with high heating rate and

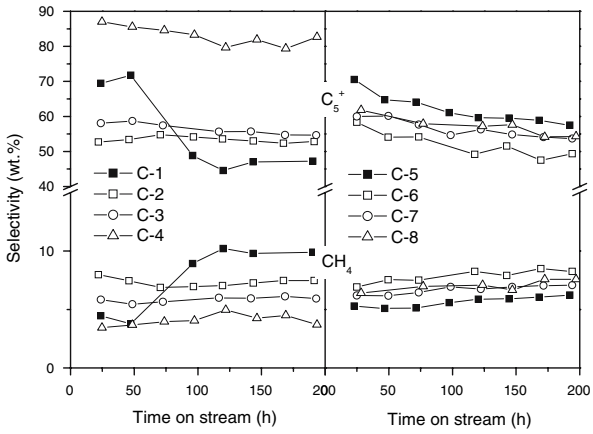

Figure 3. CH_4 and C_5^+ selectivities of the catalysts. Reaction condition: $H_2/CO = 0.67$, 270 °C, 1.50 MPa and 1000 h^{-1} for 200 h.

Table 3
Effect of calcination behaviors on FTS performances of the catalysts[a]

Catalysts	C-1	C-2	C-3	C-4	C-5	C-6	C-7	C-8
Time on stream (h)	190	191	193	194	192	194	194	197
CO conversion (%)	41.5	29.3	19.7	5.9	28.2	23.5	20.2	24.0
H_2 + CO conversion (%)	43.9	34.3	24.0	8.0	31.5	27.7	24.7	28.5
Exit molar H_2/CO ratio	0.58	0.55	0.57	0.63	0.62	0.59	0.58	0.58
Extent of WGS ($P_{CO_2}P_{H_2}/(P_{CO}P_{H_2O})$)	2.2	0.89	0.72	0.52	0.91	0.85	0.71	0.71
Hydrocarbon products distribution (wt%)								
CH_4	9.9	7.5	5.9	3.7	6.2	8.3	7.1	7.6
C_2	12.3	11.6	9.3	3.8	8.9	10.9	9.7	9.7
C_3	17.3	16.1	15.7	5.4	14.1	16.6	15.4	15.0
C_4	13.3	12.0	14.4	4.4	13.3	15.0	14.1	13.5
C_5^+	47.2	52.8	54.7	82.7	57.5	49.2	53.7	54.3
Olefin/Paraffin (wt/wt)								
C_2	0.3	1.2	1.8	1.6	2.0	0.8	0.9	0.8
C_3	2.7	7.1	8.8	6.0	8.4	5.2	5.8	5.0
C_4	3.4	6.5	7.7	5.4	7.3	5.2	5.7	5.1
C_{2-4}	1.2	2.9	4.1	3.1	4.2	2.3	2.5	2.2

[a] Reaction condition: $H_2/CO = 0.67$, 1.50 MPa, 270 °C and 1000 h^{-1} for 200 h.

the catalyst calcination in argon. These perhaps due to that the low heating rate possesses high crystal deficit of iron phase, which promotes the dissociation adsorption of CO and the low stability of the catalysts (C-6, C-7 and C-8) maybe seriously affects the promotion function of Mn, and the effects of heating rate and calcination atmosphere on the Mn promotion need to be further investigated.

4. Conclusions

Calcination behaviors have significant influences on physico-chemical properties of the precipitated iron–manganese FT catalysts. Increasing calcination temperature promoted the enrichment of Mn on the catalyst surface, decreased the surface area of the catalysts, increased the crystallite size but decreased the crystal deficit of α-Fe_2O_3, as well as suppressed the reduction/carburization of the catalysts during H_2 and syngas reduction process. The increase of calcination temperature also decreased the FT activity of the catalysts, restrained the formation of CH_4 and increased C_5^+ selectivity. Appropriate calcination temperature can improve the light olefins selectivities. On the other hand, low heating rate improved the carburization and stabilized the catalyst in FT process, increased the light olefins selectivities and shifted the products to heavy hydrocarbons. In addition, calcination in argon can improve the carburization and increase the FT activity of the catalyst. An iron–manganese catalyst with lower calcination temperature, lower heating rate and calcined in argon is optimized for FT performances.

Acknowledgments

We gratefully acknowledge the financial support from National Outstanding Young Scientists Foundation of China (20625620) and National Natural Science

Foundation of China (20590361). This work was performed under the authority of Synfuels China Co., Ltd.

References

[1] H. Xiong, Y. Zhang, S. Wang and J. Li, Catal. Comm. 6 (2005) 512.
[2] W.S. Ning, N. Koizumi and M. Yamada, Catal. Comm. 8 (2007) 275.
[3] T. Herranz, S. Rojas, F.J. Pérez-Alonso, M. Ojeda, P. Terreros and J.L.G. Fierro, Appl. Catal. A: Gen. 311 (2006) 66.
[4] T. Herranz, S. Rojas, F.J. Pérez-Alonso, M. Ojeda, P. Terreros and J.L.G. Fierro, Appl. Catal. A: Gen. 308 (2006) 19.
[5] Y. Yang, H. Xiang, R. Zhang, B. Zhong and Y. Li, Catal. Today 106 (2005) 170.
[6] H. Hayakawa, H. Tanaka and K. Fujimoto, Appl. Catal. A: Gen. 310 (2006) 24.
[7] D.B. Bukur, X. Lang, D. Mukesh, W.H. Zimmerman, M.P. Rosynek and C. Li, Ind. Eng. Chem. Res. 29 (1990) 1588.
[8] N. Egiebor and W.C. Cooper, Can. J. Chem. Eng. 63 (1985) 81.
[9] K.B. Jensen and F.E. Massoth, J. Catal. 92 (1985) 109.
[10] J. Barrault and C. Renard, Appl. Catal. 14 (1985) 133.
[11] G.C. Maiti, R. Malessa and M. Baerns, Appl. Catal. 5 (1983) 151.
[12] J.J. Venter, A. Chen and M.A. Vannice, J. Catal. 117 (1989) 170.
[13] G.C. Maiti, R. Malessa, U. Löchner, H. Papp and M. Baerns, Appl. Catal. 16 (1985) 215.
[14] R. Malessa and M. Baerns, Ind. Eng. Chem. Res. 27 (1988) 279.
[15] J.L. Rankin and C.H. Bartholomew, J. Catal. 100 (1986) 526.
[16] J.L. Rankin and C.H. Bartholomew, J. Catal. 100 (1986) 533.
[17] Y. Huang, A. White, A. Walpole and D.L. Trimm, Appl. Catal. 26 (1989) 177.
[18] Y. Yang, H.W. Xiang, L. Tian, H. Wang, C.H. Zhang, Z.C. Tao, Y.Y. Xu, B. Zhong and Y.W. Li, Appl. Catal. A: Gen. 284 (2005) 105.
[19] I.S.C. Hughes, J.O.H. Newman and G.C. Bond, Appl. Catal. 30 (1987) 303.
[20] Y. Yang, H.W. Xiang, Y.Y. Xu, L. Bai and Y.W. Li, Appl. Catal. A: Gen. 266 (2004) 181.
[21] I.R. Leith and M.G. Howden, Appl. Catal. 37 (1988) 75.
[22] B. Kolk, I.R. Albers, I.R. Leith and M.G. Howden, Appl. Catal. 37 (1988) 57.
[23] D.B. Bukur, K. Okabe, M.P. Rosynek, C. Li, D. Wang, K.R.P.M. Rao and G.P. Huffman, J. Catal. 155 (1995) 353.
[24] D. Das, G. Ravichandran and D.K. Chakrabarty, Catal. Today 36 (1997) 285.
[25] M.V. Cagnoli, S.G. Marchetti, N.G. Gallegos, A.M. Alvarez, R.C. Mercader and A.A. Yeramian, J. Catal. 123 (1990) 21.
[26] T.R. Motjope, H.T. Dlamini, G.R. Hearne and N.J. Coville, Catal. Today 71 (2002) 335.
[27] S. Li, G.D. Meitzner and E. Iglesia, J. Phys. Chem. B 105 (2001) 5743.
[28] K.B. Jensen and F.E. Massoth, J. Catal. 92 (1985) 98.